

Title No. 118-M104

# Use of Nanoclays and Methylcellulose to Tailor Rheology for Three-Dimensional Concrete Printing

by AlaEddin Douba and Shiho Kawashima

*A concrete system is identified as highly printable if it can offer minimal resistance to handling while sustaining high load resistance and structural stability. One of the major complexities of three-dimensional (3D) concrete printing lies in its sensitivity to materials and equipment that varies the time among layers, hydration time, and shear history. While nanoclays are effective additives for enhancing structural buildup, methylcellulose is introduced as a secondary additive to significantly amplify the nanoclays' effect on the static yield stress while prolonging the open time between layers and increasing filament cohesiveness. The compatibility of these two systems at different contents is studied by characterizing rheological properties such as static yield stress, steady-state viscosity, and storage modulus, as well as the heat of hydration through isothermal calorimetry. The hybrid system is found to increase the static yield stress by up to 900% compared to the reference paste at only 3.0 wt.% total content by mass.*

**Keywords:** methylcellulose; nanoclays; rheology; three-dimensional (3D) concrete printing.

## INTRODUCTION

Fresh concrete used for extrusion-based three-dimensional (3D) concrete printing (3DCP) requires a thixotropic suspension that flocculates and deflocculates quickly during rest and flow, respectively.<sup>1</sup> It exhibits contradictory rheological properties such as a low viscosity with a high static yield stress, and has rapid structural buildup at rest with a high destructuration rate during flow. To realize such a complex fresh-state performance, it is essential to identify measurable printing properties and map them through rheology. Researchers thus far have identified several key printing properties such as buildability, extrudability, pumpability, shape stability, cold joints and filament breakage, and tearing and splitting.<sup>2-19</sup> These properties can be coupled based on the stage of printing in which they are measured: 1) buildability and shape stability; 2) pumpability and extrudability; 3) cold joints and filament breakage, and tearing or splitting.

To meet the complex rheological demands of 3DCP, many researchers either use retarder/accelerator systems<sup>2,17,20-23</sup> or combine multiple rheological admixtures.<sup>2,5,7,16,19,24-27</sup> However, the use of accelerators has the potential to cause the mixture to clog.<sup>10</sup> One of the main thixotropic additives suggested by researchers working in 3DCP are nanoclays (NC),<sup>5,12,16,20,26,28,29</sup> as they have been shown to increase buildability,<sup>5,11,20,28,29</sup> robustness,<sup>5</sup> and shape stability.<sup>5,15,28</sup> However, one of the drawbacks of NC in 3DCP is its relatively high water adsorption,<sup>30</sup> which can result in excessive stiffness and, in turn, filament splitting, tearing, and breakage

at higher contents, as observed by Kazemian et al.<sup>15</sup> Furthermore, the literature shows that NC addition is not enough to meet all 3DCP requirements; it has often been mixed with other additives or required the use of other supplementary binders.<sup>5,7,11,15,16,20,24-26,29</sup> Thus, it is significant to identify admixtures compatible with NC to meet the rheological demand without negatively impacting its positive effects.

## RESEARCH SIGNIFICANCE

NC and viscosity-modifying admixtures (VMAs) have become common additives used for 3DCP. However, little work has been done to examine the compatibility of these two systems and the rheological effects of mixing them at different ratios. This work examines methylcellulose (MC) as a VMA to increase the efficiency of NC in increasing the static yield stress and buildability, and shows a wide range of NC and MC that can be used to tailor the rheological response of cement paste systems.

## BACKGROUND

Of the many printing properties of interest, buildability and shape stability are often points of focus as they are significantly more influenced by rheology, rather than the printing equipment, and can govern the overall print size and critical printing height. However, shape stability characterizes the overall print performance, while the buildability is often governed by one or a few layers. Buildability can be defined as the maximum height achieved by successful layer deposition, where the deposition of an added layer causes a collapse of the bottom layers that is not caused by structural deficiency.<sup>3-6,10-13,16,19</sup> Figures 1(a) and (b) show examples of a print failure characterizing buildability, whereas in (c), the print failure is due to the print geometry and structural stability, and hence is not suitable for measuring buildability. Shape stability is governed by the deformation of the deposited layers in their pseudo-solid state (flow has not initiated), where excessive deformation leads to unstable deposition.<sup>4,5,8,11,12,15,16</sup> Critically, elastic deformation in the pseudo-solid state becomes plastic (unrecoverable) deformation due to hydration and hardening in the deformed state. In lab conditions, shape stability can be quantified as an increased difference between the actual and the theoretical print height

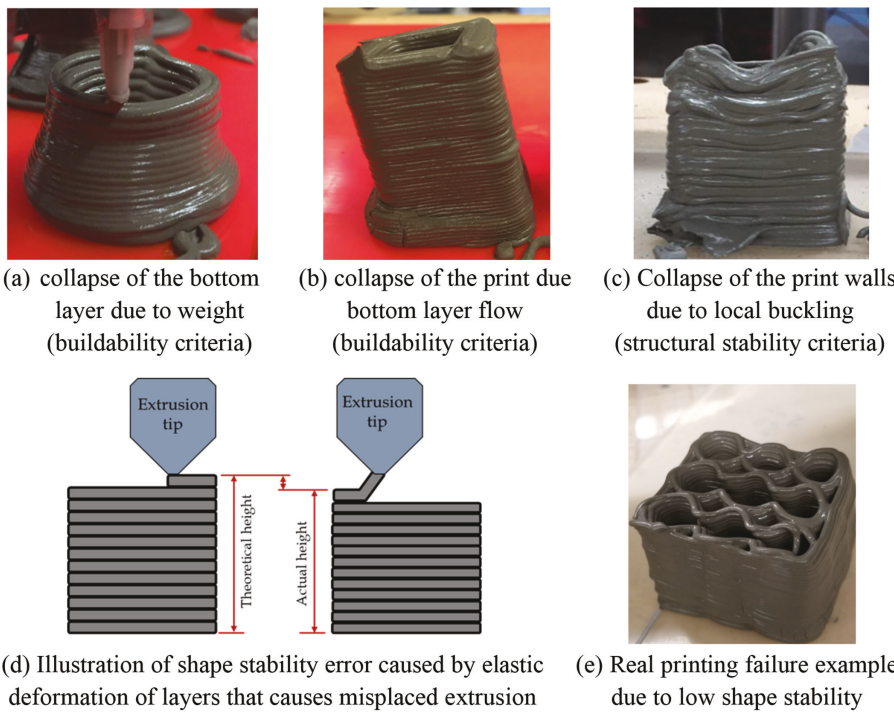


Fig. 1—Examples and illustrations of failure due to low buildability, structural instability, or low shape stability.

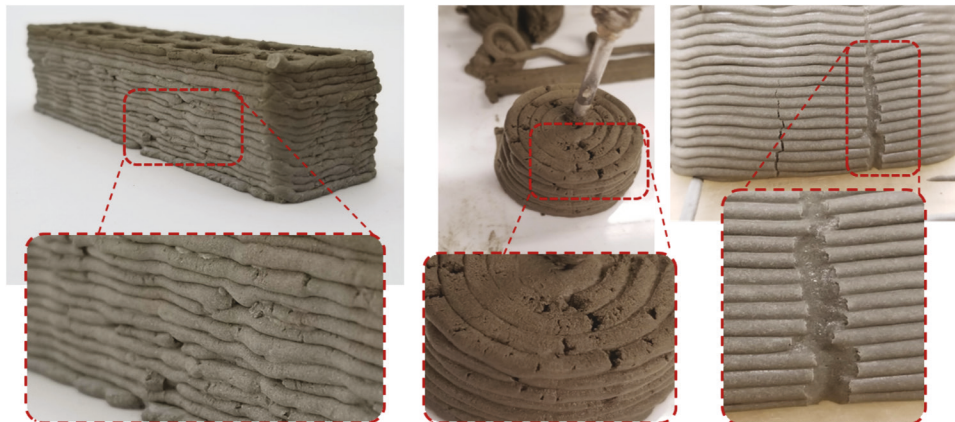


Fig. 2—Examples of filament breakage, tearing, or splitting associated with high stiffness or dryness.

(where the print integrity has not been compromised), as shown in the illustration in Fig. 1(d). An example of low shape stability is shown in Fig. 1(e).

While buildability and shape stability are often dominated by the rheological properties of the cementitious system, pumpability and extrudability are governed by the printing equipment and machinery. Pumpability and extrudability are similar in that both are characterized by the ability of the cementitious ink to flow.<sup>2,10,19</sup> Thus, they are linked to rheological properties that characterize structural breakdown, such as viscosity and dynamic yield stress. However, pumpability specifically deals with the ability to deliver the material from a feeding point to the extrusion head, while extrudability is the ability to deliver the material through and out of the extruder, both at a controlled and a desired rate.<sup>2-6,8,10,12,16,19</sup> Extrudability, therefore, has a different shear history profile than pumpability, as it is sheared for a longer time, often with less pressure and through different geometries. While printing properties such as buildability

are often characterized through rheological properties, on-site testing of the extruded material is required to ensure successful printing.<sup>18</sup> Thus, it is worth noting that despite the fact that printing properties can be defined through rheological properties and measured in the lab, field implementation remains limited due to the absence of clearly established printing tests.

Cold joints are a time-dependent weakening of the inter-layer bond strength due to the chemical incompatibility of two subsequent layers caused by unmatched hydration processes.<sup>3,7,12,14,17</sup> Unlike the other printing properties, cold joints are not always visible during printing and often can be characterized by localized reduction of the mechanical performance. Cold joints are also classified by open time: the time duration where hydration kinetics (such as initial setting or surface drying) do not interfere with the interlayer properties.<sup>4,31,32</sup> Finally, filament breakage, tearing, and splitting are often caused by excessively stiff mixtures,<sup>15</sup> unsheared centers of filament,<sup>1</sup> voids, shrinkage,

or segregation. Figure 2 shows a few examples of filament tearing, splitting, and breakage exhibited by cement paste with different rheological properties. Filament tearing, splitting, and breakage are distinguished from low extrudability as the latter is characterized by the viscosity and dynamic yield stress, while the former is governed by stiffness, cohesion, and water adsorption. Furthermore, changing the extrusion properties such as the nozzle shape, size, or rate do not resolve the errors causing splitting or tearing. Nevertheless, these properties can overlap, as an increase in the viscosity, for instance, can be correlated to increased cohesiveness, segregation resistance, and bleeding resistance.<sup>33,34</sup>

Because NC alone may not be able to meet the complex and demanding rheological profile of 3DCP, some researchers have combined NC with either a VMA<sup>5,7,25,26</sup> or a high-range water-reducing admixture (HRWRA).<sup>16,24,26</sup> VMAs in 3DCP were mainly a low molecular weight and introduced at small contents up to 1.0 wt.%, and were aimed more toward reducing segregation.<sup>7,35,36</sup> Cellulose-based VMAs are specifically of interest as they can prevent segregation due to their water retention abilities,<sup>37-39</sup> which scales with molecular weight and dosage.<sup>39</sup> However, the addition of a VMA can be unfavorable for 3DCP, as, at low contents, it can decrease the static yield stress,<sup>6,36,40</sup> increase air content,<sup>36</sup> and may decrease the compressive strength.<sup>36</sup> The addition of a cellulose-based VMA at a higher content or at a high molecular weight, however, can cause an increase in the static yield stress.<sup>41</sup> More importantly, the addition of a VMA increases cohesiveness due to the VMA binding effect on the mixing water.<sup>42</sup> Nevertheless, the pathways in which VMA polymers such as cellulose ethers (CE) affect the rheology of cement paste are still under investigation,<sup>37,43</sup> but polymer-cement interactions have been considered to originate in competitive adsorption.<sup>44</sup>

CE are six-membered D-glucose or dextrose ether rings linked together covalently by ether groups through glycosidic bonds.<sup>45</sup> The effects of CE are highly dependent on their dilution status. Polymers in dilute solutions are likely coiled up and do not have any global interaction as each coil is physically distant from the other,<sup>46</sup> resulting in solely localized effects. In semi-dilute solutions, local or global 3D networks of polymers exist, and the crossover between dilute and semi-dilute states is denoted as the critical overlapping concentration (COC).<sup>41,43,46</sup> Before the COC, the effects on the viscosity are minor and grow exponentially after reaching the COC.<sup>41</sup> Decoiling polymers due to high shear strain can significantly impact the COC, and local details of the polymer gain further influence over their behavior.<sup>43</sup> However, it has been suggested that the dependency of the COC on the strain rate is only valid for a linear polymer where highly branched polymers' COC show little correlation to the strain rate.<sup>47</sup> Because CE are linear polymers,<sup>45</sup> the dependency of rheological interactions on shear history<sup>1</sup> is of greater complexity for cement pastes containing CE due to the additional effects of the shear history on the COC. For example, Brumaud et al. discussed that the addition of high molecular weight CE could cause the collapse of the van der Waals forces network, as it generates steric repulsive forces to separate cement particles,<sup>41</sup> in a similar mechanism to

that of HRWRAs.<sup>48</sup> The adaptation of CE in cement systems also often leads to retardation effects.<sup>49-52</sup> This is caused by polymer adsorption to cement grains<sup>49,51</sup> and, more specifically, on silicate oxides and metal oxides,<sup>50,52</sup> that translates to high adsorption on C-S-H and calcium hydroxide.<sup>51</sup> More severe retardation effects are observed with a lower molecular weight<sup>52</sup> and lower degree of substitution.<sup>53</sup> Such retardation effects can be significant in increasing interlayer open time and preventing the formation of cold joints during printing.

In addition to NC and VMAs, HRWRAs such as polycarbonate ethers (PCE) might be necessary to ensure pumpability. PCEs weaken the flocculation bonding and disband the microstructure.<sup>24,54</sup> Thus, it is critical to ensure that both additives' effects on cement composites satisfy buildability, shape stability, cold joints, and cohesion, and are compatible with PCEs. Qian and De Schutter studied the compatibility between NC and PCE and showed that while PCEs present steric hindrance, NC still provides increased cohesion and static yield stress while maintaining a low dynamic yield stress.<sup>24</sup> This is attributed to the increased cohesion between flocs and the reagglomeration of the microstructure caused by the addition of NC.<sup>24</sup> Cellulose-based VMAs have also been shown to be compatible with PCE HRWRAs,<sup>55,56</sup> which, similar to NC, have been attributed to increased linking of flocs and reagglomeration.<sup>57</sup>

This study focuses on the compatibility of cellulose-based VMAs, namely MC, with NC. The rheological properties of different NC-MC hybrid systems containing up to 1.5 wt.% NC and 2.0 wt.% MC are examined, along with their effect on hydration kinetics through isothermal calorimetry. While the rheological work is solely focused on cement paste systems, it is useful to highlight that the addition of aggregate is expected to increase the static yield stress.<sup>16,58</sup> The thixotropy of cement pastes originates from soft colloidal forces—that is, van der Waals and ionic, alongside rigid forces from C-S-H bridging.<sup>59-62</sup> In this work, all early hydrate products are referred to as C-S-H links for simplicity. Unlike plain cement systems where only cement-cement interactions exist, the system introduced in this paper has additional NC-cement, NC-NC, MC-cement, MC-MC, and MC-NC interactions of both soft and rigid types. The goal of this work is to highlight the hybridization of NC and MC as a new tailorabile additive system for 3DCP applications while also examining some of the corresponding interaction mechanisms. However, because of the large number of different interactions present, isolating each of the previously listed interactions is outside the scope of this work.

## EXPERIMENTAL METHODS

### Materials

To prepare the cement paste, Type I/II cement with the chemical composition shown in Table 1 was used and mixed with distilled water at a 0.34 water-cement ratio (*w/c*). Highly purified attapulgite clay, or palygorskite, and a high-performance thixotropic rheology modifier and ant-settling agent were used in this study as the source of the NC with chemical compositions shown in Table 1. They are geometrically homogeneous needle-like particles with 30 nm

**Table 1—Chemical composition of cement**

	Content, %								Loss on ignition	
	SiO <sub>2</sub>	Al <sub>2</sub> O <sub>3</sub>	Fe <sub>2</sub> O <sub>3</sub>	CaO	MgO	SO <sub>3</sub>	P <sub>2</sub> O <sub>5</sub>			
Cement	19.06	5.01	2.27	62.55	2.93	3.31		2.84		
Nanoclays	55.2	12.2	4.05	0.49	1.98	8.56	0.68	0.53	0.62	15.66

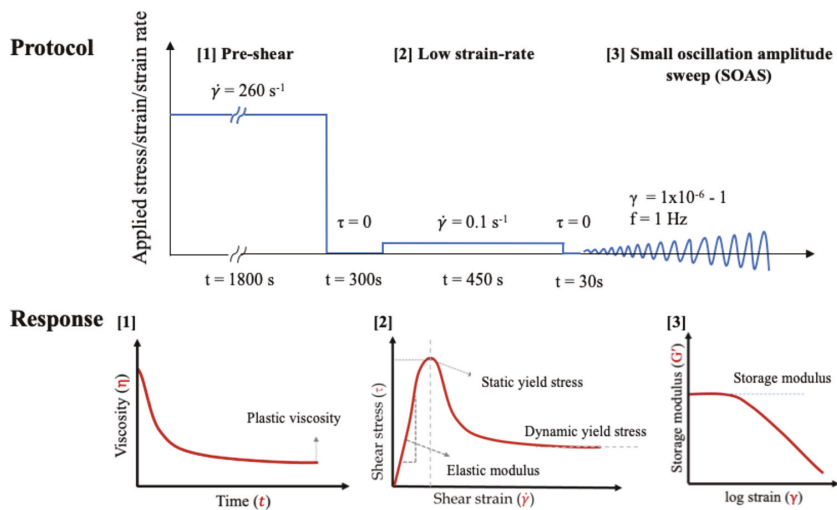


Fig. 3—Applied rheological protocol and corresponding material response measuring plastic viscosity, static yield stress, elastic modulus, dynamic yield stress, and storage modulus.

diameter, 1.5 to 2.0  $\mu\text{m}$  length, and are negatively charged along their length and positively at their ends.<sup>6</sup> The VMA was a CE, where the cellulose backbone has methoxy substitution between 27.5 and 31.5 wt.% at a degree of substitution (DS) between 1.5 and 1.9, a 50 mg/mL  $\text{H}_2\text{O}$  solubility, and a molecular weight of 14,000. The NC was dispersed in solution through magnetic stirring at 0.1, 0.5, 1.0, or 1.5 wt.% while the VMA was premixed as a powder with cement manually at 0.1, 0.5, 1.0, 1.5, or 2.0 wt.%, where both were added as weight substitution of cement. NC solutions were prepared using distilled water and stirred at 800 rpm for a minimum of 1 hour; they were mixed with cement immediately after stirring to prevent any possible sedimentation. The different cement pastes are designated based on their respective content of NC or MC, while the reference paste with no additives is referred to as Neat. For example, 1.0NC represents an addition of 1.0 wt.% NC, and 0.1MC represents an addition of 0.1 wt.% MC, both as replacement of cement by weight.

### Rheological characterization

Steady-shear and small-amplitude oscillatory shear (SAOS) rheology were used to characterize the effects of NC and MC on the rheological properties of cement pastes. A four-blade vane with a 21.9 mm blade width and a 26.6 mm inner diameter cup were used, where the gap between the vane and the bottom of the cup was 8 mm. All test specimens were prepared using fresh solutions and time-controlled mixing procedures, ensuring similar hydration and shear history prior to performing rheological measurements. Cement and MC powder (if used) were mixed by hand for 30 seconds, then the NC solution or distilled water was added

to the mixture. One hundred and fifty seconds after the first contact between the water/solution and powder, the mixture was mixed at 500 rpm for 2 minutes. Then, the paste was loaded into the rheometry cup and the cup was loaded into the rheometer. Lastly, the vane was inserted into the sample 6 minutes after mixing was complete, and the rheological protocol was initiated 30 seconds after vane insertion.

All measurements were made on a stress-controlled rheometer at a controlled temperature of 25°C. A pre-shear of 260 1/s was applied for 30 minutes to ensure all mixtures reached a deflocculated reference state, followed by a rest period of 5 minutes to allow for structural buildup. The plastic viscosity, defined as the viscosity reached after shear thinning under constant shear, was measured during the steady-state response at the end of the pre-shear. Following the rest period, a strain of 0.1 1/s was applied for 7.5 minutes, where both the static and dynamic yield stresses were determined. The static yield stress is defined as the stress needed for the initial flow of the material, making the transition from solid-like to liquid-like behavior. The dynamic yield stress is the minimum stress required to maintain the state of flow after the static yield stress has been achieved, or the stress needed to terminate flow. Another rest period of 30 seconds was applied, followed by a SAOS strain sweep from  $1 \times 10^{-6}$  to 1 at 1 Hz to measure the storage modulus. The storage modulus is the elastic, in-phase response of a viscoelastic material subjected to an oscillatory shear within the linear viscoelastic regime. This was measured after the static yield stress to minimize the number of tests due to the high number of mixtures examined in this study. A minimum of four freshly prepared pastes were tested per mixture, and up to eight when the variance was greater than 10%. The

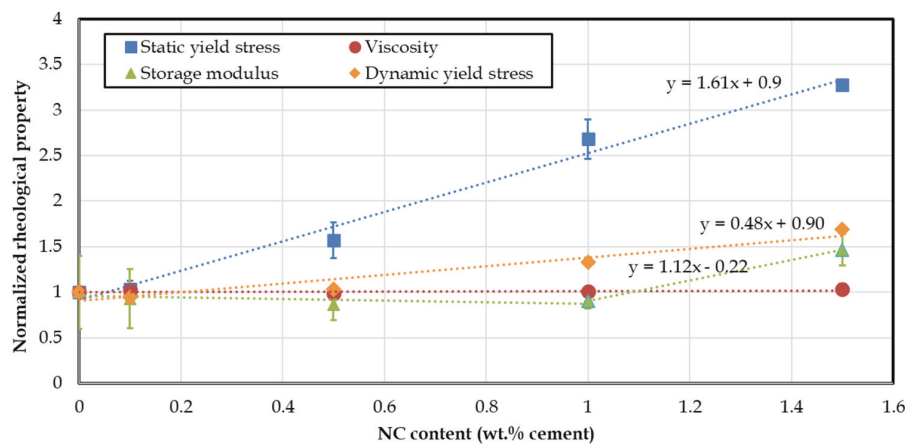


Fig. 4—Rheological properties of cement paste containing NC normalized by rheological properties of Neat cement with static yield stress of 249 Pa, dynamic yield stress of 49 Pa, viscosity of 1.59 Pa·s, and storage modulus of 0.26 MPa.

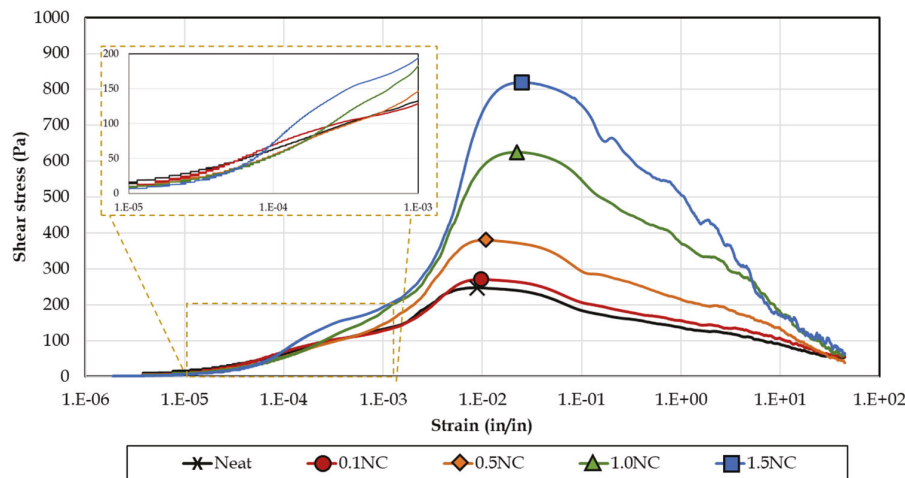


Fig. 5—Stress-strain response of cement paste containing NC during static yield stress measurement where point of flow initiation (peak stress) is marked accordingly.

rheological testing protocol and the corresponding material response characterizing rheological properties are illustrated in Fig. 3.

### Isothermal calorimetry

The effects of the hybrid additives on cement hydration kinetics were monitored using an isothermal calorimeter. Cement paste mixtures were prepared following the same procedure prescribed for rheological characterization, and a 5 g sample was measured and loaded into a standardized glass ampule. Data collection started 5 to 10 minutes from mixing, the temperature was kept at 25°C, and a total of 6000 data points were collected over 48 to 72 hours.

## RESULTS AND DISCUSSION

### Rheology of NC cement pastes

To best characterize the interaction between both MC and NC systems, cement pastes with either NC or MC alone were examined first to isolate the effect of each additive on the rheological properties. Figure 4 shows the relative rheological properties of cement pastes using NC alone with respect to the Neat cement paste containing no additives. Similar to findings by other researchers and previous

studies, the addition of NC significantly increases the static yield stress of cement paste proportionally to NC content with no increase in the viscosity.<sup>15,33,63-65</sup> Further, the increase in the static yield stress is over three times that of the increase in the dynamic yield stress, supporting the suitability of NC for 3DCP with high buildability and ease of pumpability.<sup>5,12,16,20,26,28,29</sup> There is no significant change in the storage modulus with the addition of NC up to 1.0 wt.% content. Increasing the content to 1.5 wt.%, however, leads to an increase of the storage modulus by 46%. Roussel et al.<sup>59</sup> indicate that the static yield stress in cement paste systems finds its origin in rigid C-S-H links and soft colloidal interactions. In contrast, the storage modulus is a feature dominated by the rigid network. The stress response at strain levels in 1E-2 ~ 1E+0 is associated with the soft network, whereas the stress response in the range 1E-5 ~ 1E-3 corresponds to the rigid network.<sup>59</sup>

The stress-strain response of cement pastes containing only NC is shown in Fig. 5. The markers indicate the point of flow onset characterizing the static yield stress, and the corresponding strain is referred to as the critical strain. Clearly, the increase in the static yield stress, which scales with the NC dosage, is significantly higher than the change

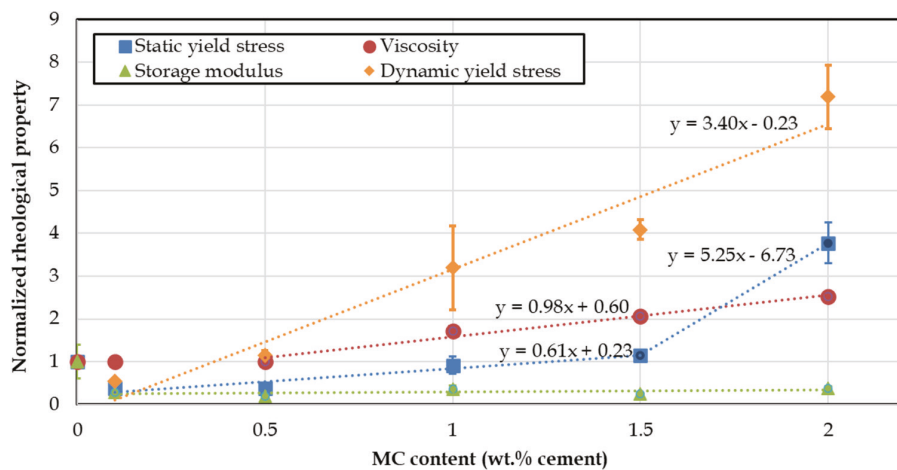


Fig. 6—Rheological properties of cement paste containing only MC normalized by Neat cement with static yield stress of 249 Pa, dynamic yield stress of 49 Pa, viscosity of 1.59 Pa·s, and storage modulus of 0.26 MPa.

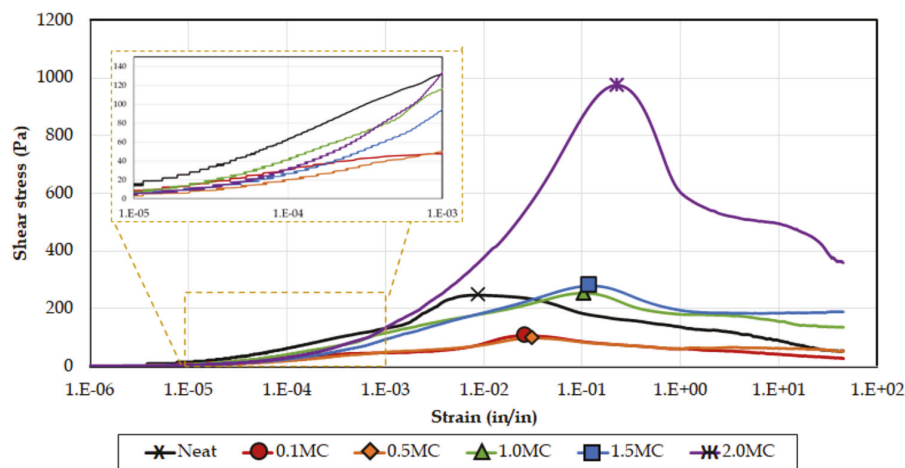


Fig. 7—Stress-strain response of cement paste containing MC during static yield stress measurement where point of flow initiation (peak stress) is marked accordingly.

in the critical strain. This in turn implies a stiffer colloidal network due to the addition of NC. Further analysis shows that at lower strain levels, specifically in the range  $1\text{E-}5 \sim 1\text{E-}4$ , the stress levels remain close to that of the reference cement independently of the NC dosage. At strain levels in the range of  $1\text{E-}4 \sim 1\text{E-}3$ , there is an increase in the stress response compared to the Neat cement paste proportional to the NC content. This suggests that the effects of the NC on the rigid network are minimal up to 1.0 wt.% NC content, which agrees with the storage modulus results. Thus, the changes in the static yield stress can be inferred from the soft colloidal network, specifically NC-NC and NC-cement interactions, which is in agreement with findings from other studies.<sup>57</sup>

### Rheology of MC cement pastes

The rheological properties of the cement paste containing only MC were measured and are shown in Fig. 6 with respect to the Neat cement. The addition of 0.1 wt.% MC shows a decrease in the static yield stress, dynamic yield stress, and storage modulus, with insignificant changes to the viscosity. The storage modulus of the cement paste with MC is independent of the MC dosage up to 2.0 wt.%, showing an overall decrease and softening of the rigid network compared to the

Neat. These results agree with the findings of Brumaud et al., where they showed significant softening of cement paste at low strains.<sup>41</sup> The decrease in the storage modulus can be attributed to the adsorption of polymers on cement grains and hydration products.<sup>49-52</sup> An addition of MC beyond 0.1 wt.% results in an increase in the viscosity and dynamic yield stress proportional to the MC content. At 0.5 wt.% MC, the viscosity and dynamic yield stress are statistically indifferent to that of the Neat paste. Chen et al. reported similar behavior using hydroxypropyl MC (HPMC), where flowability did not change significantly at low contents but was significantly reduced at higher contents.<sup>34</sup> Similarly, the static yield stress increases with an increase in the MC content from 0.5 wt.% MC, reaching a 280% increase at 2.0 wt.% compared to the Neat paste. Similar findings were reported by Brumaud et al. using hydroxyethyl MC (HEMC), showing a decrease at lower contents and then increase with increasing content by up to ~300%.<sup>41</sup> However, a shift in efficiency is observed at approximately a 1.5 wt.% dosage, where the efficiency between 1.5 and 2.0 wt.% is 8.6 times higher than that between 0.1 and 1.5 wt.%, which can be attributed to reaching the COC, signaling the formation of a global 3D network of elongated polymer chains.<sup>41,43,46</sup>

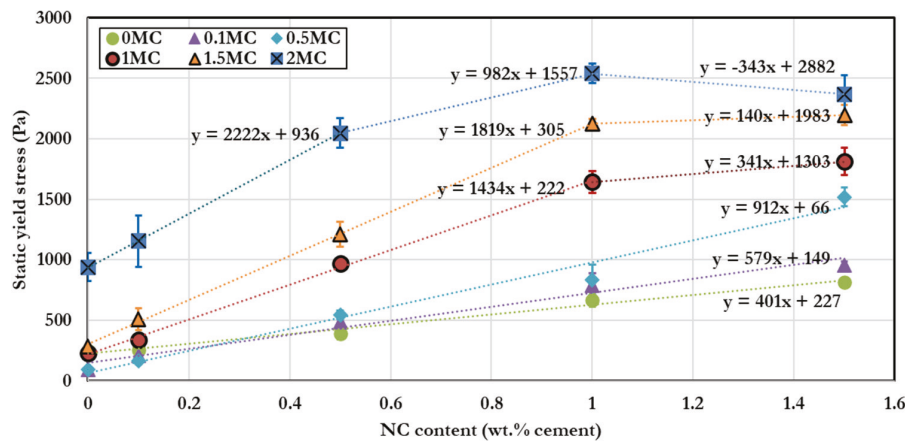


Fig. 8—Static yield stress of cement paste incorporating NC and MC with respect to NC content.

The stress-strain response during static yield stress measurements was recorded and is shown in Fig. 7. The addition of MC shows a significant increase of the critical strain in the range of 1E-2 ~ 1E+0 compared to the Neat paste, which agrees with the findings of Brumaud et al.<sup>41</sup> The addition of MC up to 1.5 wt.% causes little to no change in the static yield stress and a significant increase in the strain, which indicates relaxation of the soft colloidal network. MC polymers can be coiled up within a suspension, especially at dosages lower than the COC. The introduction of the shear strain rate can cause polymer chains to uncoil, orient, or stretch parallel to the driving force.<sup>66,67</sup> Thus, relaxation within cement colloidal networks containing MC can be attributed to the stretching of polymer chains, similar to the observation of Ma and Kawashima on diutan gum.<sup>57</sup> Further, all the MC mixtures show a significantly lower stress response at 1E-5 ~ 1E-3 strain compared to the Neat paste, implying further relaxation of the rigid network in agreement with measurements of the storage modulus. However, this relaxation could also be attributed to the collapse of the van der Waals network<sup>41</sup> or increased steric hindrance.<sup>57</sup> The low static yield stress with the addition of MC up to 1.5 wt.%, along with the significant increase in the dynamic yield stress and plastic viscosity, has an overall undesirable effect for 3DCP. In fact, recovering the loss in the static yield stress observed at 0.1 wt.% requires increasing the MC dosage to 1.0 wt.%, which causes an increase in the dynamic yield stress and viscosity by 219% and 65%, respectively. At 2.0 wt.%, where the addition of MC reaches a 280% increase in the static yield stress, the corresponding increase in the dynamic yield stress and plastic viscosity are 639% and 151%, respectively. Therefore, it is evident that, rheologically, MC alone is unfavorable in enhancing the printability of cement paste. Still, the addition of MC as a VMA for 3DCP can improve segregation and bleeding resistance and increase cohesiveness,<sup>7,33-36</sup> thus offering advantageous properties for 3DCP that NC do not.

### Rheology of hybrid NC-MC cement pastes

**Static yield stress**—It was observed that the addition of NC causes an increase in the static yield stress proportional to the NC content, while the addition of MC shows a higher static yield stress than that of the Neat paste only at dosages greater than 1.5 wt.%. Incorporating both NC and MC as

a hybrid additive, however, leads to different behavior than NC or MC alone on the static yield stress of cement paste, as shown in Fig. 8. The addition of NC alone results in NC efficiency of 400 Pa per 1 wt.% NC (measured by the slope of the linear regression line). The combination of NC and MC further enhances NC efficiency, reaching 2222 Pa per 1 wt.% NC at 2.0 wt.% MC, which is almost five times the efficiency of NC alone. However, a critical NC concentration is observed at an MC dosage of 1.0 wt.% or higher, where the increased NC efficiency is diminished or receded. The critical NC concentration seems to be inversely proportional to the MC content, which could imply that at certain high dosages, there are competing effects of soft and rigid interactions between NC, MC, and cement.

Nevertheless, there is a significant overall increase in the static yield stress with the addition of MC compared to the mixtures incorporating NC alone. For example, at 2.0 wt.% MC and 1.5 wt.% NC, the increase in the static yield stress is 190% higher than 1.5 wt.% NC alone, despite the diminished NC efficiency. Up to such critical concentration, the increase in the NC efficiency is proportional to the MC dosage: a 900 Pa increase in the static yield stress per 1 wt.% NC, per 1 wt.% MC, as shown in Fig. 9. This significant increase in the NC efficiency on the static yield stress can produce cement paste with a static yield stress of 2540 Pa at 2 wt.% MC and 1.0 wt.% NC, which is a 920% increase from that of the Neat paste. In fact, to achieve a similar increase using NC alone, 5.77 wt.% NC is required, which is a 477% increase in the NC dosage compared to the addition of only 2.0 wt.% MC. The significantly higher static yield stress in the hybrid system compared to NC or MC alone can be explained by increased NC-NC, NC-cement, MC-cement, new NC-MC interactions, or increased MC-MC interactions that replicate the formation of the MC global network at the COC.

**Plastic viscosity**—The addition of MC leads to an increase in the viscosity from 0.5 to 2.0 wt.% proportional to the MC content, whereas the addition of NC alone does not change the viscosity of cement paste up to a 1.5 wt.% content. For hybrids at 0.1 wt.% MC, the change in the viscosity is statistically indifferent to the NC content or pastes with NC alone; and at 0.5 wt.% MC or greater, there is an increase in the viscosity proportional to the NC content, as shown in Fig. 10. The increase in the plastic viscosity due to NC

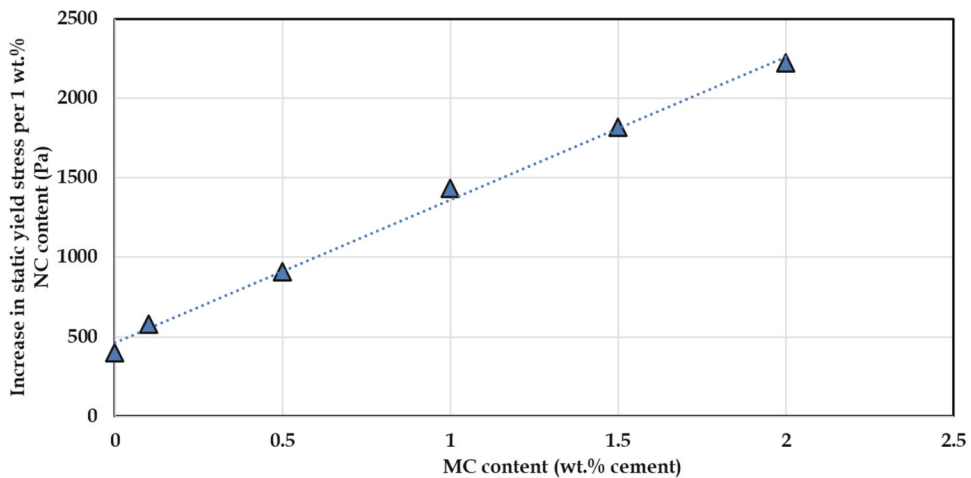


Fig. 9—NC efficiency change with respect to MC content measured by increase in static yield stress per 1 wt. % NC content.

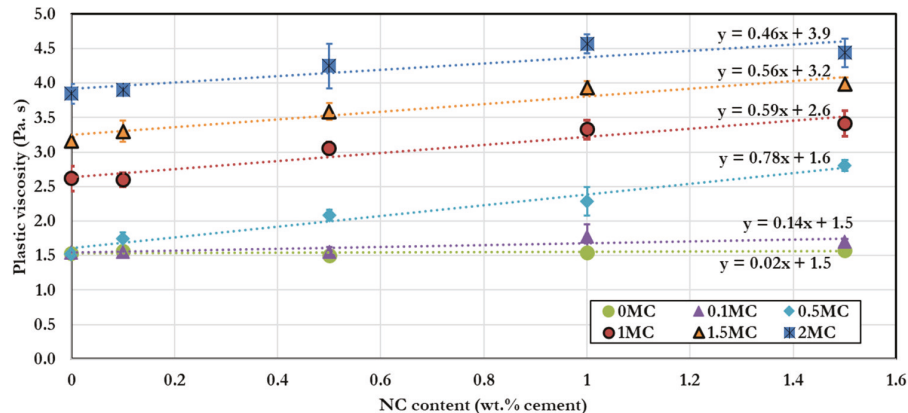


Fig. 10—Plastic viscosity of cement paste incorporating both NC and MC.

addition is within 0.46 to 0.78 Pa·s per 1 wt.% NC, which corresponds to a 16 to 84% increase from their respective pastes containing only MC, or an 83 to 190% increase from the Neat paste. While such an increase can be considered significant, it is accompanied by a more significant increase in the static yield stress in the range of 511 to 920%. Furthermore, other researchers have reported successful printing using cement mixtures with viscosities in the range of 3.5 to 4.5 Pa·s,<sup>11</sup> which are similar to the maximum viscosities reported herein, or significantly higher viscosities up to 33 Pa·s.<sup>19</sup> It is also important to note that while a high viscosity harms pumpability, a low viscosity can also lead to segregation.<sup>10</sup> Nevertheless, the newly found increase in viscosity in hybrids with relation to the NC content implies a new type of interaction between NC and MC that is proportional to the NC content, namely NC-MC. The mechanisms of such interaction and their relationship to other NC-cement, NC-NC, MC-MC, and MC-cement interactions are outside the scope of this investigation.

**Dynamic yield stress**—The results showed that the addition of NC and MC alone causes an increase in the dynamic yield stress per their respective contents, where MC has a significantly higher efficiency than NC. The effect of NC and MC addition results in an increase in the dynamic yield stress proportional to the NC content up to 1.0 wt.%, as shown in Fig. 11, at a much higher efficiency than NC or MC alone.

Similar to the plastic viscosity, the addition of 0.1 wt.% MC is statistically indifferent from the effects of the NC addition alone. However, the NC efficiency in increasing the dynamic yield stress is not consistently proportional to the MC content, in contrast to the static yield stress. For example, the NC efficiency at 1.5 wt.% MC is lower than that of 1.0 and 2.0 wt.%, and there are critical NC concentrations at MC contents of 1.0 wt.% or greater, where the NC efficiency is diminished or receded. The authors hypothesize that the COC of MC could be affected by new NC-MC interactions. However, this remains outside of the scope of this investigation and will be the subject of future work.

The dynamic yield stress is characterized by structural breakdown rather than buildup (which is the case in the static yield stress)<sup>68</sup> and hence can be used as an indicator of dynamic stability. A high yield stress has been correlated to displaying high segregation resistance.<sup>69,70</sup> Thus, ensuring that the dynamic yield stress is not too low can ensure increased segregation resistance. On the other hand, if the applied pumping shear stress required to meet the dynamic yield stress exceeds the segregation stress, water bleeding and segregation behavior arise.<sup>10</sup> Thus, the dynamic yield stress must be maintained within a range that is not too high to hinder pumping or too low to cause segregation. Researchers have reported successful printing with cement systems displaying dynamic yield stresses of up to 490,<sup>19</sup>

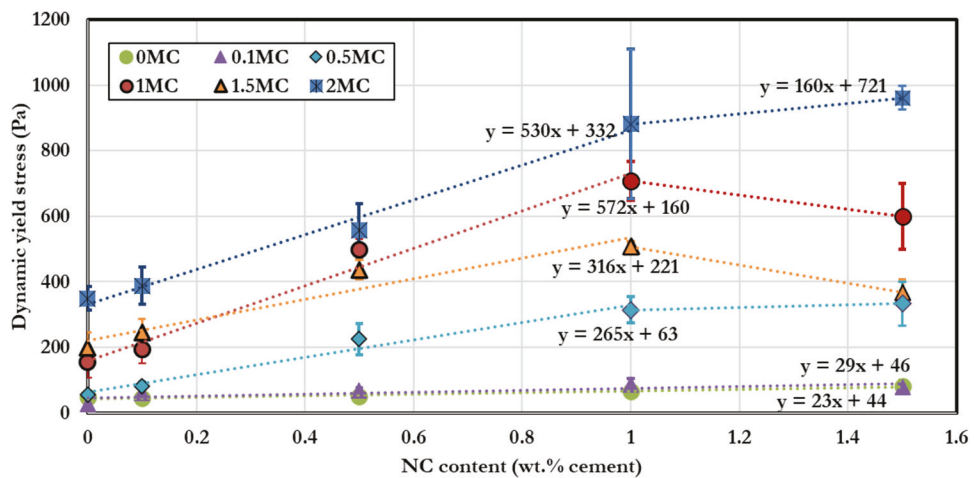


Fig. 11—Dynamic yield stress of cement paste incorporating both NC and MC.

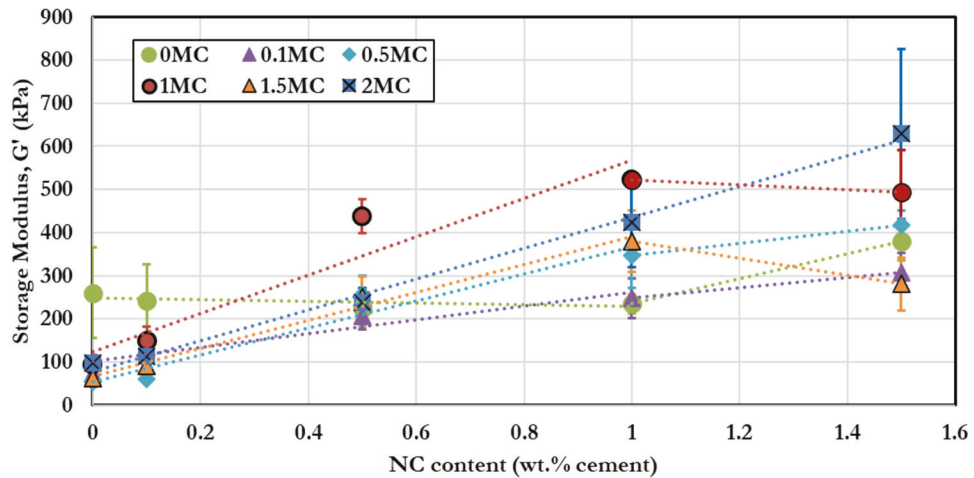


Fig. 12—Storage modulus of cement paste incorporating both NC and MC with respect to NC content.

645,<sup>27</sup> and 720 Pa.<sup>23</sup> While the hybrid additives significantly increase the dynamic yield stress, they remain within workable range except for 1.0 and 1.5 wt.% NC at 2.0 wt.% MC, which are also sensitive to the pumping equipment.

**Storage modulus**—It was previously shown that the storage modulus of the cement paste decreases with the addition of MC irrespective of content (Fig. 6). It was also shown that the storage modulus incorporating NC is similar to that of the reference paste up to 1.0 wt.% and then increases at 1.5 wt.% (Fig. 4). As a result, the two NC regions are separated by presenting the full storage modulus results in Fig. 12 and plotting the slopes of the NC efficiency between 0 and 1 wt.% and 1 and 1.5 wt.% NC in Fig. 13. The addition of NC into the MC-cement system, where the NC content is between 0 and 1 wt.%, shows an increase in the storage modulus compared to MC alone, proportional to the NC content (Fig. 12), and the NC efficiency scales with the MC content (Fig. 13). The increase in the storage modulus is high enough that at 0.5 wt.% NC content all the MC mixtures recover the loss in the storage modulus caused by the MC addition. At 1.0 wt.% NC and MC dosages of 0.5 wt.% or higher, there is a further increase in the storage modulus, showing higher values than the Neat paste. Between 1 and 1.5 wt.% NC, all mixtures maintain a higher storage modulus

than the Neat paste. However, the relationship between MC content and the NC efficiency is negative, excluding the MC dosage of 2.0 wt.%. At 1 and 1.5 wt.% MC, further addition of NC results in a decrease in the storage modulus when increasing the NC content from 1 to 1.5 wt.%. On the other hand, the NC efficiency at 2.0 wt.% MC maintains similar NC efficiency between both regions, which can be attributed to reaching the COC.

The increase in the storage modulus is an indication of a strengthened rigid network. Because the addition of MC does not cause an increase in the storage modulus, as shown in Fig. 6, the increase in the storage modulus of many hybrid mixtures compared to the Neat paste likely is not attributable to increased MC-cement but rather to increased NC-cement or cement-cement interactions. As hybrid mixtures can exhibit a higher storage modulus than mixtures with NC alone, incorporating MC could improve the NC-cement rigid interactions. Such is likely combined with a decrease in the MC processes that causes a decrease in the storage modulus. Furthermore, the dependency of the NC efficiency on the NC dosage region and COC observed in Fig. 13 implies that some competitive adsorption or interactions may be at play between the NC and MC. The origin of this requires

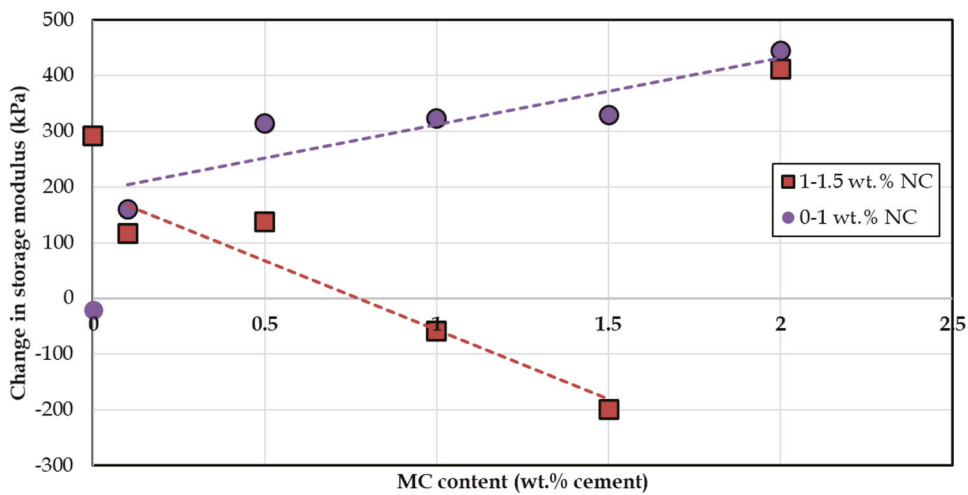


Fig. 13—NC efficiency measured as slope of regression lines in Fig. 12.

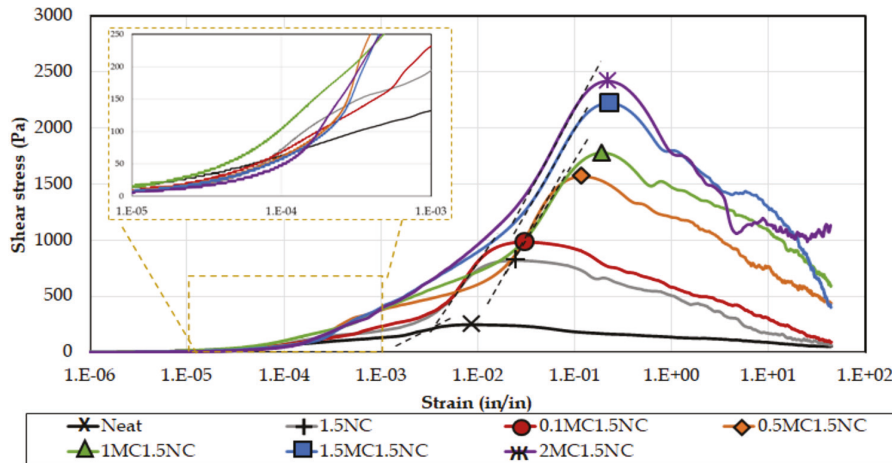


Fig. 14—Stress-strain response of cement paste at 1.5 wt. % NC and varying MC content during static yield stress measurements.

more detailed rheological probing and will be the topic of future work.

**Stress-strain response**—To further characterize the effect of hybridization and the addition of MC and NC on cement paste, the stress-strain response was examined during measurements of the static yield stress, the results of which are shown in Fig. 14. Due to the high number of mixtures, only 1.5 wt.% NC is shown, and the response at different MC dosages is examined. As noted previously, there is an increase in the NC efficiency in increasing the static yield stress that scales with the MC content, resulting in a significantly higher static yield stress than 1.5 wt.% NC alone. Higher MC content shows an increase in the critical strain, similar to the behavior observed in pastes containing MC alone (Fig. 7). However, the increase in the critical strain in the range of  $1E-2 \sim 1E+0$  is associated with an increase in the static yield stress and thus does not reflect relaxation of the colloidal network. Instead, the increase in the critical strain could be attributed to stretching of the polymer chains<sup>57,66,67</sup> or bridging between flocculation.<sup>41</sup> The stress response at lower strains  $1E-5 \sim 1E-3$  shows a similar response to systems with NC alone (Fig. 5) instead of systems with MC alone, where the stress is not significantly different from that of the Neat in the range of  $1E-5 \sim 1E-4$  and is higher

at strains in the range of  $1E-4 \sim 1E-3$ . However, no clear correlation between the stress response within  $1E-4 \sim 1E-3$  and the MC content is observed, indicating that it is likely that a mixture of interactions is occurring.

The rigid network governed by C-S-H forces ruptures at strains in the range of  $(1E-5 \sim 1E-3)$ .<sup>59</sup> Hence, the stiffness of the colloidal network can be quantified by measuring the slope of the linear stress-strain response prior to reaching the onset of flow at strains within  $(1E-2 \sim 1E+0)$ , as shown by the dotted lines in Fig. 14. The colloidal elastic modulus for all the mixtures was measured similarly and the results are shown in Fig. 15. Evidently, the addition of NC significantly increases the elastic modulus up to 190% at 0 wt.% MC, where the Neat cement already exhibits a relatively high elastic modulus due to the low *w/c*. Such an increase can lead to very dry extruded layers with significant filament tearing or splitting, as shown in Fig. 2 and observed by Kazemian et al.<sup>15</sup> The addition of MC, on the other hand, significantly reduces the colloidal elastic modulus by up to 96% at 1.0 wt.% MC, which can compromise shape stability and cause excessive elastic deformation, as presented in Fig. 1(d) and (e). The addition of NC into MC increases the colloidal elastic modulus proportionally to the NC content (at any given MC dosage). This increases ranges between

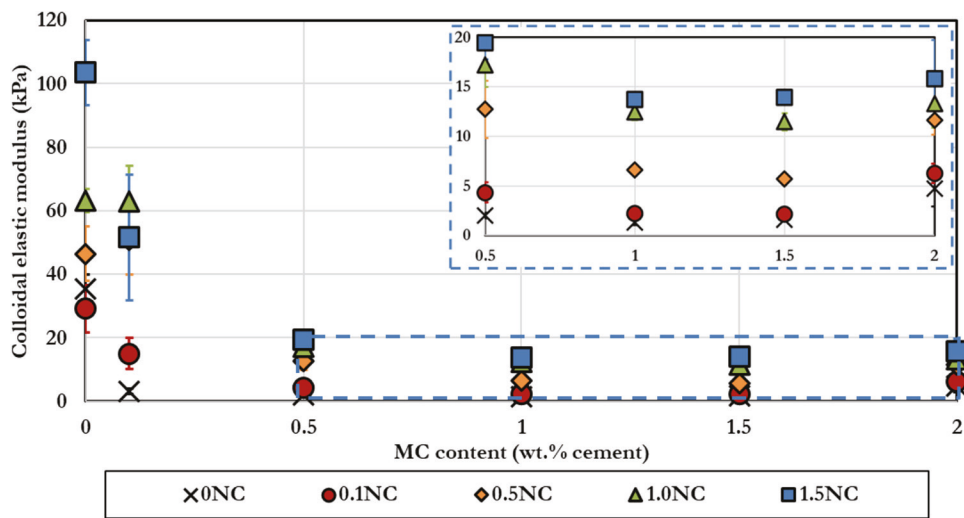


Fig. 15—Colloidal stiffness measured by slopes of linear stress-strain response prior to reaching static yield stress, shown by dotted lines in Fig. 14 for illustrations.

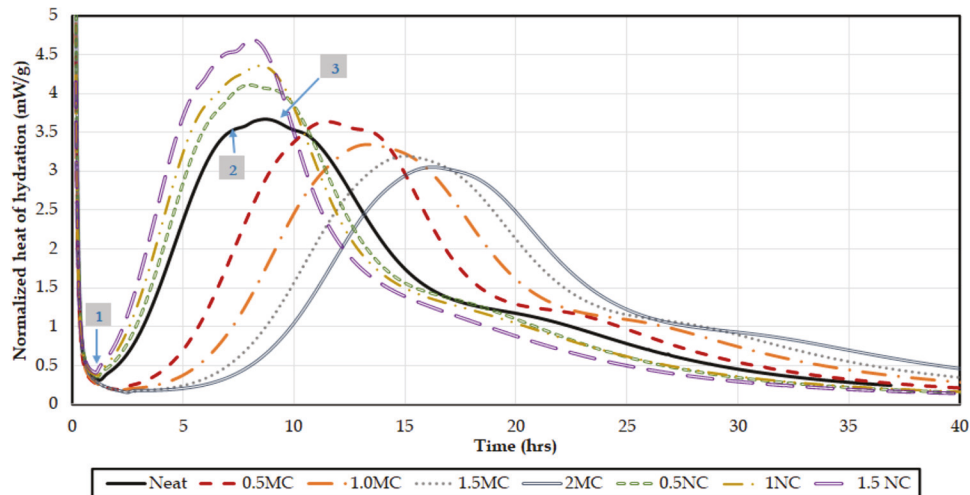


Fig. 16—Heat of hydration measured by isothermal calorimetry for cement pastes containing only either MC or NC. Point 1 marks termination peak and end of dormant period.<sup>71-73</sup> Points 2 and 3 together mark acceleration period and are associated with main C3S and C3A reactions, respectively.<sup>72,74</sup>

235% and 2000% at 2.0 and 0.1 wt.% MC, respectively, resulting in elastic modulus values between those of NC or MC alone. This can translate to maintaining shape stability while simultaneously minimizing possible filament tearing due to increased cohesiveness.

*Isothermal calorimetry*—To analyze the effects of NC and MC on hydration kinetics, isothermal calorimetry was used to record the heat of hydration. For systems containing only NC or MC, the results are shown in Fig. 16, in which three critical points are identified. Point 1 marks the termination peak and the end of the dormant period<sup>71-73</sup> and is associated with the initial setting,<sup>74</sup> which impacts the open time and interlayer properties such as the formation of cold joints. Points 2 and 3 together mark the peak and end of the acceleration period and are associated with the main C3S and C3A reactions, respectively.<sup>72,74</sup> Evidently, NC and MC display opposite effects on the hydration kinetics of cement paste. The addition of NC alone results in an increase in the heat of hydration during the acceleration period, while the addition

of MC alone causes a decrease, both proportionally to their respective content. The time of the termination peak does not change significantly with the addition of NC; however, it is severely prolonged due to the addition of MC and can last up to 6 to 8 hours at 2.0 wt.% MC. Such retardation has been reported by other researchers and is attributed to the polymer adsorption on cement grains, specifically silicate oxides and metal oxides,<sup>49-52</sup> causing delays in C-S-H formation and further adsorption onto C-S-H and calcium hydroxide.<sup>51</sup> The retardation effect of MC, however, is lower than other CE, such as HPMC, HEMC, and hydroxyethyl cellulose (HEC).<sup>52</sup> Nevertheless, the delay in the time to the termination peak further delays the time of the acceleration period, causing delays in the final set and initial hardening. The authors postulate that it hinders the rate of structuration and, therefore, buildability.

The heat of hydration curves of the mixtures containing 1.5 wt.% NC and different dosages of MC are shown in Fig. 17. This hybrid mixture was selected because it

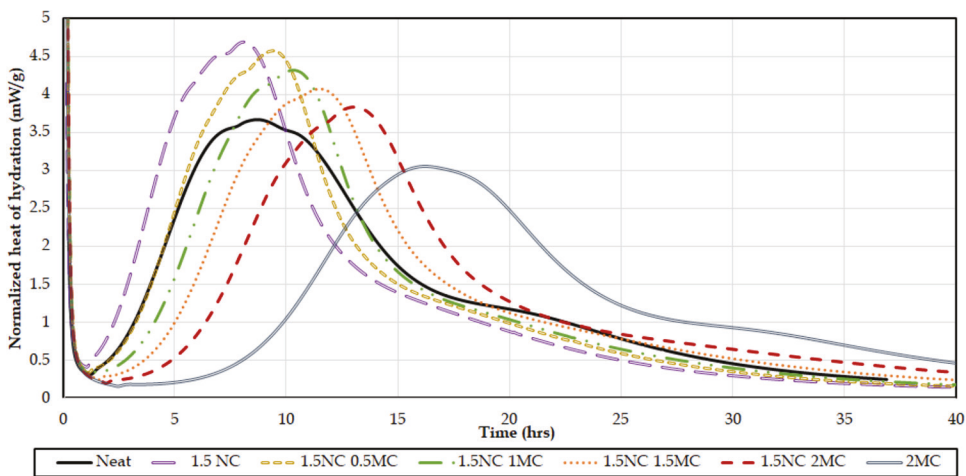


Fig. 17—Heat of hydration measured by isothermal calorimetry at 1.5 wt. % NC and different MC dosages.

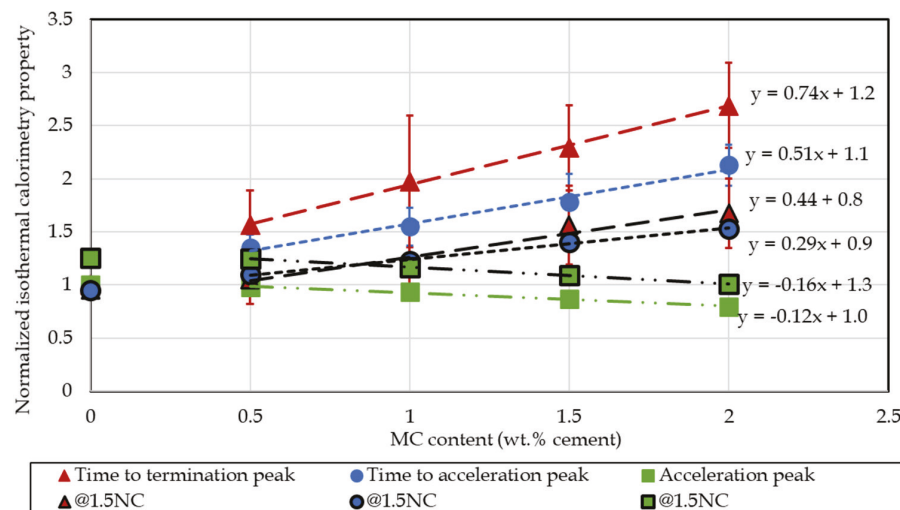


Fig. 18—Maximum heat of acceleration peak and time to acceleration and termination peaks normalized by corresponding values of Neat paste where peak heat is 3.68 mW/g, time to maximum heat of acceleration peak is 8.4 hours, and time to termination peak is 1.0 hour.

represents the boundaries of how NC and MC affect hydration kinetics. As observed from measuring the maximum heat of hydration of the acceleration peak and the time to both the acceleration and termination peaks, the hydration properties are proportional to the respective NC or MC dosages, as shown in Fig. 18. Previous rheological results showed that the effects of hybridization of NC and MC are not always linear, resulting, for instance, in a critical NC concentration in the static yield stress or mixed behavior in the storage modulus measurements between 0 and 1 wt.% and 1 and 1.5 wt.%. In contrast, calorimetry shows that the effects on hydration kinetics are linear and additive between NC and MC at all contents. The addition of NC reduces the retardation effects of MC, marked by the decreased slopes of time to acceleration and termination peaks by 40% and 43%, respectively. Furthermore, the addition of NC reduces the relative time between both peaks by 50%, thus maintaining the desired prolonged open time with fewer adverse effects on the time of the acceleration peak. For example, at 2.0 wt.% MC and 1.5 wt.% NC, the maximum heat of the acceleration peak is reached at 11.1 hours, which is only a 32% delay compared with an increase of the open time by 70% from

that of the reference paste. The maximum heat of the acceleration peak is also recovered with the addition of NC with MC. Further, at 2 wt.% MC and 1.5 wt.% NC the decrease in the heat of hydration from MC is completely negated by the increase due to the addition of NC. These results imply that an NC:MC ratio of 3:4 or greater is required to mitigate and balance the adverse retardation effects of MC.

## CONCLUSIONS

Nanoclays (NC) are an important rheological additive in improving the static yield stress of cement systems with minimal effects on the plastic viscosity or dynamic yield stress. However, they often cause a significant increase in stiffness that leads to filament tearing, require a significantly high dosage if used alone, and cannot increase the dynamic stability or ensure cohesiveness or bleeding resistance. Viscosity-modifying admixtures (VMAs) such as methylcelulose (MC) contribute to many of the drawbacks expressed by NC systems by increasing ink cohesion; however, their effect on rheology and hydration kinetics when used alone can be unfavorable. In this work, the effects of combining

both NC and MC on cement paste systems were studied and showed that:

1. The addition of MC into NC cement paste systems increases the NC efficiency by 900 Pa per 1 wt.% MC compared to the addition of NC alone, increasing the static yield stress by up to 900% compared to the reference paste with no additives (Neat paste).

2. NC alone increase the colloidal stiffness by up to 190%, producing highly stiff mixtures causing filament tearing. In contrast, MC decreases it by up to 96%, resulting in soft deformable filaments. Therefore, both impair shape stability. Results indicate hybridization can make it possible to maintain stiffness values that are neither too high nor too low.

3. The measurements of the plastic viscosity of the hybrid system reveal new types of interactions that scale proportionally to both NC and MC contents, and the increase in the viscosity of the hybrid system remains within the pumpability range for three-dimensional concrete printing (3DCP).

4. The hybrid use of NC and MC as an admixture can increase the storage modulus of the cement paste compared to the Neat paste, indicating stronger rigid networks. More investigation is needed to better understand the underlying mechanism.

5. The adverse effect of the MC addition on hydration kinetics can be mitigated by adding NC at an NC:MC ratio of 3:4 or greater in the systems studied while maintaining a delayed termination peak time corresponding to a prolonged open time.

6. The hybrid mixture of NC and MC can offer increased buildability at significantly lower NC contents while maintaining rheological properties that correlate with high shape stability and extrudability, prolonged open time to reduce the risk of cold joint formation, and reduced filament tearing due to high stiffness.

## AUTHOR BIOS

ACI member **AlaEddin Douba** is a PhD student in the Civil Engineering and Engineering Mechanics Department at Columbia University, New York, NY. He received his BS from American University of Sharjah, Sharjah, UAE, and his MS from the University of New Mexico, Albuquerque, NM. His research interests include polymer concrete, cement and concrete rheology, and the use of nanomaterials as additives for construction binder systems.

ACI member **Shiho Kawashima** is an Associate Professor of civil engineering and engineering mechanics at Columbia University. She received her BS from Columbia University and her MS and PhD from Northwestern University, Evanston, IL. She is a member of ACI Committees 236, Material Science of Concrete; 238, Workability of Fresh Concrete; 241, Nanotechnology of Concrete; and 564, 3-D Printing with Cementitious Materials. Her research interests include cement and concrete rheology, and the use of nanomaterials in cement-based systems.

## ACKNOWLEDGMENTS

The authors would like to acknowledge the National Science Foundation (Award No. 1653419) for financial support, and technical support by the staff of Columbia University's Carleton Laboratory.

## REFERENCES

1. Roussel, N., "A Thixotropy Model for Fresh Fluid Concretes: Theory, Validation and Applications," *Cement and Concrete Research*, V. 36, No. 10, Oct. 2006, pp. 1797-1806.
2. Wangler, T.; Roussel, N.; Bos, F. P.; Salet, T. A. M.; and Flatt, R. J., "Digital Concrete: A Review," *Cement and Concrete Research*, V. 123, Sept. 2019, p. 105780. doi: 10.1016/j.cemconres.2019.105780
3. Buswell, R. A.; Leal de Silva, W. R.; Jones, S. Z.; and Dirrenberger, J., "3D Printing Using Concrete Extrusion: A Roadmap for Research," *Cement and Concrete Research*, V. 112, Oct. 2018, pp. 37-49. doi: 10.1016/j.cemconres.2018.05.006
4. Le, T. T.; Austin, S. A.; Lim, S.; Buswell, R. A.; Gibb, A. G. F.; and Thorpe, T., "Mix Design and Fresh Properties for High-Performance Printing Concrete," *Materials and Structures*, V. 45, No. 8, Aug. 2012, pp. 1221-1232.
5. Rahul, A. V.; Santhanam, M.; Meena, H.; and Ghani, Z., "3D Printable Concrete: Mixture Design and Test Methods," *Cement and Concrete Composites*, V. 97, Mar. 2019, pp. 13-23.
6. Panda, B.; Ruan, S.; Unluer, C.; and Tan, M. J., "Investigation of the Properties of Alkali-Activated Slag Mixes Involving the Use of Nanoclay and Nucleation Seeds for 3D Printing," *Composites Part B: Engineering*, V. 186, Apr. 2020, p. 107826. doi: 10.1016/j.compositesb.2020.107826
7. Mendoza Reales, O. A.; Duda, P.; Silva, E. C. C. M.; Paiva, M. D. M.; and Toledo Filho, R. D., "Nanosilica Particles as Structural Buildup Agents for 3D Printing with Portland Cement Pastes," *Construction and Building Materials*, V. 219, Sept. 2019, pp. 91-100. doi: 10.1016/j.conbuildmat.2019.05.174
8. Panda, B.; Unluer, C.; and Tan, M. J., "Extrusion and Rheology Characterization of Geopolymer Nanocomposites Used in 3D Printing," *Composites Part B: Engineering*, V. 176, Nov. 2019, p. 107290. doi: 10.1016/j.compositesb.2019.107290
9. Jo, J. H.; Jo, B. W.; Cho, W.; and Kim, J.-H., "Development of a 3D Printer for Concrete Structures: Laboratory Testing of Cementitious Materials," *International Journal of Concrete Structures and Materials*, V. 14, 2020, Article No. 13.
10. Lu, B.; Weng, Y.; Li, M.; Qian, Y.; Leong, K. F.; Tan, M. J.; and Qian, S., "A Systematic Review of 3D Printable Cementitious Materials," *Construction and Building Materials*, V. 207, May 2019, pp. 477-490. doi: 10.1016/j.conbuildmat.2019.02.144
11. Zhang, Y.; Zhang, Y.; Liu, G.; Yang, Y.; Wu, M.; and Pang, B., "Fresh Properties of a Novel 3D Printing Concrete Ink," *Construction and Building Materials*, V. 174, June 2018, pp. 263-271.
12. Roussel, N., "Rheological Requirements for Printable Concretes," *Cement and Concrete Research*, V. 112, Oct. 2018, pp. 76-85. doi: 10.1016/j.cemconres.2018.04.005
13. Bos, F.; Wolfs, R.; Ahmed, Z.; and Salet, T., "Additive Manufacturing of Concrete in Construction: Potentials and Challenges of 3D Concrete Printing," *Virtual and Physical Prototyping*, V. 11, No. 3, 2016, pp. 209-225. doi: 10.1080/17452759.2016.1209867
14. Tay, Y. W. D.; Ting, G. H. A.; Qian, Y.; Panda, B.; He, L. W.; and Tan, M. J., "Time Gap Effect on Bond Strength of 3D-Printed Concrete," *Virtual and Physical Prototyping*, V. 14, No. 1, 2019, pp. 104-113. doi: 10.1080/17452759.2018.1500420
15. Kazemian, A.; Yuan, X.; Cochran, E.; and Khoshnevis, B., "Cementitious Materials for Construction-Scale 3D Printing: Laboratory Testing of Fresh Printing Mixture," *Construction and Building Materials*, V. 145, Aug. 2017, pp. 639-647. doi: 10.1016/j.conbuildmat.2017.04.015
16. Zhang, Y.; Zhang, Y.; She, W.; Yang, L.; Liu, G.; and Yang, Y., "Rheological and Harden Properties of the High-Thixotropy 3D Printing Concrete," *Construction and Building Materials*, V. 201, Mar. 2019, pp. 278-285. doi: 10.1016/j.conbuildmat.2018.12.061
17. Dressler, I.; Freund, N.; and Lowke, D., "The Effect of Accelerator Dosage on Fresh Concrete Properties and on Interlayer Strength in Shotcrete 3D Printing," *Materials*, V. 13, No. 2, 2020, p. 374.
18. Nerella, V. N.; Krause, M.; and Mechtricherine, V., "Direct Printing Test for Buildability of 3D-Printable Concrete Considering Economic Viability," *Automation in Construction*, V. 109, Jan. 2020, p. 102986. doi: 10.1016/j.autcon.2019.102986
19. Weng, Y.; Li, M.; Tan, M. J.; and Qian, S., "Design 3D Printing Cementitious Materials via Fuller Thompson Theory and Marson-Percy Model," *Construction and Building Materials*, V. 163, Feb. 2018, pp. 600-610. doi: 10.1016/j.conbuildmat.2017.12.112
20. Soltan, D. G., and Li, V. C., "A Self-Reinforced Cementitious Composite for Building-Scale 3D Printing," *Cement and Concrete Composites*, V. 90, July 2018, pp. 1-13.
21. Wangler, T.; Lloret, E.; Reiter, L.; Hack, N.; Gramazio, F.; Kohler, M.; Bernhard, M.; Dillenburger, B.; Buchli, J.; Roussel, N.; and Flatt, R., "Digital Concrete: Opportunities and Challenges," *RILEM Technical Letters*, V. 1, 2016, pp. 67-75. doi: 10.21809/rilemttechlett.2016.16
22. Bentz, D. P.; Jones, S. Z.; Bentz, I. R.; and Peltz, M. A., "Towards the Formulation of Robust and Sustainable Cementitious Binders for 3-D Additive Construction by Extrusion," *Construction and Building Materials*, V. 175, June 2018, pp. 215-224.
23. Chen, M.; Li, L.; Wang, J.; Huang, Y.; Wang, S.; Zhao, P.; Lu, L.; and Cheng, X., "Rheological Parameters and Building Time of 3D Printing Sulphoaluminate Cement Paste Modified by Retarder and Diatomite," *Construction and Building Materials*, V. 234, Feb. 2020, p. 117391. doi: 10.1016/j.conbuildmat.2019.117391

24. Qian, Y., and De Schutter, G., "Enhancing Thixotropy of Fresh Cement Pastes with Nanoclay in Presence of Polycarboxylate Ether Superplasticizer (PCE)," *Cement and Concrete Research*, V. 111, Sept. 2018, pp. 15-22.

25. Charrier, M., and Ouellet-Plamondon, C., "Testing Procedures on Materials to Formulate the Ink for 3D Printing," *Transportation Research Record: Journal of the Transportation Research Board*, V. 2674, No. 2, Feb. 2020, pp. 21-32. doi: 10.1177/0361198120907583

26. Sajadi, S. M.; Boul, P. J.; Thaemlitz, C.; Meiyazhagan, A. K.; Puthirath, A. B.; Tiwary, C. S.; Rahman, M. M.; and Ajayan, P. M., "Direct Ink Writing of Cement Structures Modified with Nanoscale Additive," *Advanced Engineering Materials*, V. 21, No. 8, Aug. 2019, p. 1801380. doi: 10.1002/adem.201801380

27. Chen, M.; Liu, B.; Li, L.; Cao, L.; Huang, Y.; Wang, S.; Zhao, P.; Lu, L.; and Cheng, X., "Rheological Parameters, Thixotropy and Creep of 3D-Printed Calcium Sulfoaluminate Cement Composites Modified by Bentonite," *Composites Part B: Engineering*, V. 186, Apr. 2020, p. 107821. doi: 10.1016/j.compositesb.2020.107821

28. Panda, B.; Lim, J. H.; and Tan, M. J., "Mechanical Properties and Deformation Behaviour of Early Age Concrete in the Context of Digital Construction," *Composites Part B: Engineering*, V. 165, May 2019, pp. 563-571.

29. Panda, B., and Tan, M. J., "Experimental Study on Mix Proportion and Fresh Properties of Fly Ash Based Geopolymer for 3D Concrete Printing," *Ceramics International*, V. 44, No. 9, June 2018, pp. 10258-10265.

30. Kawashima, S.; Kim, J. H.; Corr, D. J.; and Shah, S. P., "Study of the Mechanisms Underlying the Fresh-State Response of Cementitious Materials Modified with Nanoclays," *Construction and Building Materials*, V. 36, Nov. 2012, pp. 749-757.

31. Paul, S. C.; van Zijl, G. P. A. G.; Tan, M. J.; and Gibson, I., "A Review of 3D Concrete Printing Systems and Materials Properties: Current Status and Future Research Prospects," *Rapid Prototyping Journal*, V. 24, No. 4, 2018, pp. 784-798.

32. Nerella, V. N.; Hempel, S.; and Mechtherine, V., "Effects of Layer-Interface Properties on Mechanical Performance of Concrete Elements Produced by Extrusion-Based 3D-Printing," *Construction and Building Materials*, V. 205, Apr. 2019, pp. 586-601. doi: 10.1016/j.conbuildmat.2019.01.235

33. Liu, Y.; Han, J.; Li, M.; and Yan, P., "Effect of a Nanoscale Viscosity Modifier on Rheological Properties of Cement Pastes and Mechanical Properties of Mortars," *Construction and Building Materials*, V. 190, Nov. 2018, pp. 255-264.

34. Kovler, K., and Roussel, N., "Properties of Fresh and Hardened Concrete," *Cement and Concrete Research*, V. 41, No. 7, July 2011, pp. 775-792. doi: 10.1016/j.cemconres.2011.03.009

35. Chen, Y.; Figueiredo, S. C.; Li, Z.; Chang, Z.; Jansen, K.; Çopuroğlu, O.; and Schlangen, E., "Improving Printability of Limestone-Calcined Clay-Based Cementitious Materials by Using Viscosity-Modifying Admixture," *Cement and Concrete Research*, V. 132, June 2020, p. 106040.

36. Grabiec, A. M., "Influence of Viscosity Modifying Agent on Some Rheological Properties, Segregation Resistance and Compressive Strength of Self-Compacting Concrete," *Journal of Civil Engineering and Management*, V. 19, No. 1, 2013, pp. 1-8.

37. Brumaud, C.; Bessaies-Bey, H.; Mohler, C.; Baumann, R.; Schmitz, M.; Radler, M.; and Roussel, N., "Cellulose Ethers and Water Retention," *Cement and Concrete Research*, V. 53, Nov. 2013, pp. 176-184.

38. Patural, L.; Porion, P.; Van Damme, H.; Govin, A.; Grosseau, P.; Ruot, B.; and Devès, O., "A Pulsed Field Gradient and NMR Imaging Investigations of the Water Retention Mechanism by Cellulose Ethers in Mortars," *Cement and Concrete Research*, V. 40, No. 9, Sept. 2010, pp. 1378-1385.

39. Patural, L.; Marchal, P.; Govin, A.; Grosseau, P.; Ruot, B.; and Devès, O., "Cellulose Ethers Influence on Water Retention and Consistency in Cement-Based Mortars," *Cement and Concrete Research*, V. 41, No. 1, Jan. 2011, pp. 46-55.

40. Benaicha, M.; Roguiez, X.; Jalbaud, O.; Burtschell, Y.; and Alaoui, A. H., "Influence of Silica Fume and Viscosity Modifying Agent on the Mechanical and Rheological Behavior of Self Compacting Concrete," *Construction and Building Materials*, V. 84, June 2015, pp. 103-110. doi: 10.1016/j.conbuildmat.2015.03.061

41. Brumaud, C.; Baumann, R.; Schmitz, M.; Radler, M.; and Roussel, N., "Cellulose Ethers and Yield Stress of Cement Pastes," *Cement and Concrete Research*, V. 55, Jan. 2014, pp. 14-21.

42. Khayat, K. H., "Workability, Testing, and Performance of Self-Consolidating Concrete," *ACI Materials Journal*, V. 96, No. 3, May-June 1999, pp. 346-353.

43. Prakash, J. R., "Universal Dynamics of Dilute and Semidilute Solutions of Flexible Linear Polymers," *Current Opinion in Colloid & Interface Science*, V. 43, Oct. 2019, pp. 63-79.

44. Bessaies-Bey, H.; Baumann, R.; Schmitz, M.; Radler, M.; and Roussel, N., "Organic Admixtures and Cement Particles: Competitive Adsorption and Its Macroscopic Rheological Consequences," *Cement and Concrete Research*, V. 80, Feb. 2016, pp. 1-9.

45. Nasatto, P. L.; Pignon, F.; Silveira, J. L. M.; Duarte, M. E. R.; Noseda, M. D.; and Rinaudo, M., "Methylcellulose, a Cellulose Derivative with Original Physical Properties and Extended Applications," *Polymers*, V. 7, No. 5, May 2015, pp. 777-803.

46. Bessaies-Bey, H.; Palacios, M.; Pustovgar, E.; Hanafi, M.; Baumann, R.; Flatt, R. J.; and Roussel, N., "Non-Adsorbing Polymers and Yield Stress of Cement Paste: Effect of Depletion Forces," *Cement and Concrete Research*, V. 111, Sept. 2018, pp. 209-217.

47. Papanagopoulos, D.; Pierri, E.; and Dondos, A., "Influence of the Shear Rate, of the Molecular Architecture and of the Molecular Mass on the Critical Overlapping Concentration  $c^*$ ," *Polymer*, V. 39, No. 11, 1998, pp. 2195-2199.

48. Flatt, R., and Schober, I., "Superplasticizers and the Rheology of Concrete," *Understanding the Rheology of Concrete*, N. Roussel, ed., Woodhead Publishing Series in Civil and Structural Engineering, Sawston, UK, 2012, pp. 144-208.

49. Young, J. F., "A Review of the Mechanisms of Set-Retardation in Portland Cement Pastes Containing Organic Admixtures," *Cement and Concrete Research*, V. 2, No. 4, July 1972, pp. 415-433. doi: 10.1016/0008-8846(72)90057-9

50. Baba, T., and Tsujimoto, Y., "Examination of Calcium Silicate Cements with Low-Viscosity Methyl Cellulose or Hydroxypropyl Cellulose Additive," *BioMed Research International*, V. 2016, 2016, p. 4583854. doi: 10.1155/2016/4583854

51. Pourchez, J.; Grosseau, P.; and Ruot, B., "Changes in C3S Hydration in the Presence of Cellulose Ethers," *Cement and Concrete Research*, V. 40, No. 2, 2010, pp. 179-188. doi: 10.1016/j.cemconres.2009.10.008

52. Ou, Z. H.; Ma, B. G.; and Jian, S. W., "Influence of Cellulose Ethers Molecular Parameters on Hydration Kinetics of Portland Cement at Early Ages," *Construction and Building Materials*, V. 33, Aug. 2012, pp. 78-83. doi: 10.1016/j.conbuildmat.2012.01.007

53. Weyer, H. J.; Müller, I.; Schmitt, B.; Bosbach, D.; and Putnis, A., "Time-Resolved Monitoring of Cement Hydration: Influence of Cellulose Ethers on Hydration Kinetics," *Nuclear Instruments and Methods in Physics Research Section B: Beam Interactions with Materials and Atoms*, V. 238, No. 1-4, Aug. 2005, pp. 102-106.

54. Qian, Y.; Lesage, K.; El Cheikh, K.; and De Schutter, G., "Effect of Polycarboxylate Ether Superplasticizer (PCE) on Dynamic Yield Stress, Thixotropy and Flocculation State of Fresh Cement Pastes in Consideration of the Critical Micelle Concentration (CMC)," *Cement and Concrete Research*, V. 107, May 2018, pp. 75-84.

55. Kawai, T., and Okada, T., "Effect of Superplasticizer and Viscosity-Increasing Admixture on Properties of Lightweight Aggregate Concrete," *Superplasticizers and Other Chemical Admixtures in Concrete*, SP-119, V. M. Malhotra, ed., American Concrete Institute, Farmington Hills, MI, Sept. 1989, pp. 583-604.

56. Palacios, M., and Flatt, R. J., "Working Mechanism of Viscosity-Modifying Admixtures," *Science and Technology of Concrete Admixtures*, P.-C. Aitcin and R. J. Flatt, eds., Woodhead Publishing, Sawston, UK, 2016, pp. 415-432.

57. Ma, S., and Kawashima, S., "Investigating the Working Mechanisms of Viscosity-Modifying Admixtures through Rheological and Water Transport Properties," *Journal of Materials in Civil Engineering*, ASCE, V. 32, No. 2, Feb. 2020, p. 4019357. doi: 10.1061/(ASCE)MT.1943-5533.0003018

58. Ivanova, I., and Mechtherine, V., "Effects of Volume Fraction and Surface Area of Aggregates on the Static Yield Stress and Structural Build-Up of Fresh Concrete," *Materials*, V. 13, No. 7, Apr. 2020, p. 1551. doi: 10.3390/ma13071551

59. Roussel, N.; Ovarlez, G.; Garrault, S.; and Brumaud, C., "The Origins of Thixotropy of Fresh Cement Pastes," *Cement and Concrete Research*, V. 42, No. 1, Jan. 2012, pp. 148-157.

60. Coussot, P., "Introduction to the Rheology of Complex Fluids," *Understanding the Rheology of Concrete*, N. Roussel, ed., Woodhead Publishing Series in Civil and Structural Engineering, Sawston, UK, 2012, pp. 3-22.

61. Flatt, R. J., "Dispersion Forces in Cement Suspensions," *Cement and Concrete Research*, V. 34, No. 3, Mar. 2004, pp. 399-408. doi: 10.1016/j.cemconres.2003.08.019

62. Flatt, R. J., and Bowen, P., "Electrostatic Repulsion between Particles in Cement Suspensions: Domain of Validity of Linearized Poisson-Boltzmann Equation for Nonideal Electrolytes," *Cement and Concrete Research*, V. 33, No. 6, June 2003, pp. 781-791. doi: 10.1016/S0008-8846(02)01059-1

63. Dejaeghere, I.; Sonebi, M.; and De Schutter, G., "Influence of Nano-Clay on Rheology, Fresh Properties, Heat of Hydration and Strength of

Cement-Based Mortars," *Construction and Building Materials*, V. 222, Oct. 2019, pp. 73-85.

64. Qian, Y., and Kawashima, S., "Use of Creep Recovery Protocol to Measure Static Yield Stress and Structural Rebuilding of Fresh Cement Pastes," *Cement and Concrete Research*, V. 90, Dec. 2016, pp. 73-79.

65. Ma, S.; Qian, Y.; and Kawashima, S., "Experimental and Modeling Study on the Non-Linear Structural Build-Up of Fresh Cement Pastes Incorporating Viscosity Modifying Admixtures," *Cement and Concrete Research*, V. 108, June 2018, pp. 1-9. doi: 10.1016/j.cemconres.2018.02.022

66. Bhardwaj, P.; Kamil, M.; and Panda, M., "Surfactant-Polymer Interaction: Effect of Hydroxypropylmethyl Cellulose on the Surface and Solution Properties of Gemini Surfactants," *Colloid and Polymer Science*, V. 296, No. 11, Nov. 2018, pp. 1879-1889. doi: 10.1007/s00396-018-4409-5

67. Zhang, J. Y.; Wang, X. P.; Liu, H. Y.; Tang, J. A.; and Jiang, L., "Interfacial Rheology Investigation of Polyacrylamide-Surfactant Interactions," *Colloids and Surfaces A: Physicochemical and Engineering Aspects*, V. 132, No. 1, Jan. 1998, pp. 9-16. doi: 10.1016/S0927-7757(97)00151-9

68. Abebe, Y. A., and Lohaus, L., "Rheological Characterization of the Structural Breakdown Process to Analyze the Stability of Flowable Mortars under Vibration," *Construction and Building Materials*, V. 131, Jan. 2017, pp. 517-525. doi: 10.1016/j.conbuildmat.2016.11.102

69. Saak, A. W.; Jennings, H. M.; and Shah, S. P., "New Methodology for Designing Self-Compacting Concrete," *ACI Materials Journal*, V. 98, No. 6, Nov.-Dec. 2001, pp. 429-439.

70. Assaad, J.; Khayat, K. H.; and Daczko, J., "Evaluation of Static Stability of Self-Consolidating Concrete," *ACI Materials Journal*, V. 101, No. 3, May-June 2004, pp. 207-215.

71. Makar, J. M., and Chan, G. W., "Growth of Cement Hydration Products on Single-Walled Carbon Nanotubes," *Journal of the American Ceramic Society*, V. 92, No. 6, June 2009, pp. 1303-1310.

72. Makar, J. M., and Chan, G. W., "End of the Induction Period in Ordinary Portland Cement as Examined by High-Resolution Scanning Electron Microscopy," *Journal of the American Ceramic Society*, V. 91, No. 4, Apr. 2008, pp. 1292-1299. doi: 10.1111/j.1551-2916.2008.02304.x

73. Makar, J. M.; Chan, G. W.; and Esseghaier, K. Y., "A Peak in the Hydration Reaction at the End of the Cement Induction Period," *Journal of Materials Science*, V. 42, No. 4, Feb. 2007, pp. 1388-1392.

74. Mindess, S.; Young, J. F.; and Darwin, D., *Concrete*, Prentice Hall, Upper Saddle River, NJ, 2003, 671 pp.

Reproduced with permission of copyright owner. Further reproduction  
prohibited without permission.